Available online at www.sciencedirect.com

SciVerse ScienceDirect

Energy Procedia 30 (2012) 116 – 124

Energy Procedia

SHC 2012

A model of the optical properties of a non-absorbing media with application to thermotropic materials for overheat protection

Adam Gladen[a], Jane H. Davidson[a], Susan C. Mantell[a]*, Jihua Zhang[b] , Yuewen Xu[b]

[a]*Department of Mechanical Engineering, University of Minnesota, 111 Church St SE, Minneapolis 55455, USA*
[b]*Department of Chemistry, University of Minnesota, 207 Pleasant St SE, Minneapolis 55455, USA*

Abstract

Thermotropic materials offer the potential to provide overheat protection for polymer absorbers. These materials are composed of a matrix material in which a second material, referred to as the scattering domain, is dispersed. Temperature control is accomplished by a reduction in transmittance at a desired temperature corresponding to the phase change temperature of the scattering domain. The phase change is accompanied by a change in refractive index. This paper describes a numerical model to predict the transmittance and reflectance of a polymer based thermotropic material as a function of the relative index of refraction *m* between the matrix and scattering domains, the scattering domain size and volume fraction f_v, and the sheet thickness. The thermotropic material is modelled as a non-absorbing sheet comprised of discrete anisotropic scattering spherical particles embedded in a matrix material. Under the assumption that the particles scatter incident radiation independently, the direction of scattered radiation is determined by Mie theory. A Monte Carlo numerical technique is used to predict the transmittance and reflectance for thermotropic materials in which the matrix index of refraction is 1.5 (representative of polymers) and the incident wavelength is 550 nm. Model results are validated by comparison to measured transmittance for 0.3 mm thick polymer samples containing particles with 200 nm radius at *m* ranging from 0.97 to 1.09 and f_v ranging from 5 to 18.2%. As the mismatch in refractive indices and volume fraction increase, the transmittance is reduced. For example, the transmittance is reduced from 83% for m=1.02 and f_v = 9.6 to approximately 50% for m=1.09 and f_v =13.5% (200 nm radius and 0.3 mm thick).

* Corresponding author. Tel.: +011-612-625-1324; fax: +011-612-625-6069.
E-mail address: smantell@umn.edu.

doi:10.1016/j.egypro.2012.11.015

Keywords: Thermotropic material; Monte Carlo simulation; radiation scattering

1. Introduction

One of the hindrances to the wide scale adoption of distributed solar thermal collectors for domestic hot water is the payback period required to recoup the initial cost of the system [1-3]. Solar domestic hot water (SDHW) collectors constructed of polymers offer the potential to reduce the initial cost [1-4]. A challenge to the development of a glazed polymeric SDHW collector is the potential of the absorber to overheat [5, 6]. Thermotropic materials could provide passive overheat protection [5, 6] because the transmittance, reflectance, and/or absorptance depend on temperature [7, 8]. For polymer SDHW collector applications, it is proposed that the thermotropic material is clear (i.e. high transmittance and low reflectance) below the absorber overheat temperature limit. As the absorber temperature approaches the maximum allowed working temperature, the thermotropic material switches to a state of low transmittance and high reflectance, thus providing overheat protection. The state of low transmittance is referred to as the translucent state.

The physical mechanism by which thermotropic materials change from the clear state to the translucent state varies [6-8]. For example, in phase change thermotropic materials, also referred to as thermotropic materials with fixed domains, discrete particles are embedded in a matrix material. The refractive indices of the two materials match in the clear state. As the material is heated, the refractive index of the particles changes, often due to a phase change, which creates a mismatch between the refractive index of the matrix and the particle. The mismatch in refractive index scatters radiation [6-8]. Regardless of the physical mechanism for switching from the clear state to the translucent, all thermotropic materials in the translucent state rely on particles with an index of refraction different from the index of refraction of the matrix material to scatter radiation. If the radiation is back scattered, then the reflectance of the material will increase and the transmittance will decrease. To date thermotropic materials have been considered for various applications such as thermal overheat protection of polymer SDHW collectors [6, 9] and thermal regulation of interior spaces through fenestration applications [7, 8, 10, 11].

The objective of this study is to examine the effects of particle size, refractive index of the particle, volume fraction of the particles, and the thickness of the layer on the normal-hemispherical transmittance and reflectance of a thermotropic material. Normal hemispherical transmittance and reflectance are referred to as transmittance and reflectance unless otherwise noted. Previous research has examined the effects of particle size for a laminate sample comprised of a glass layer and a thermotropic layer of fixed thickness [12]. The effect of volume fraction of glass spheres in polymer films less than 300 um thick has also been studied for infrared wavelengths [13, 14]. A parametric study of particle size and index of refraction in the ranges and wavelength applicable for thermotropic materials for passive overheat protection has yet to be performed.

In the present study, a model was created to determine the transmittance and reflectance of a thermotropic material. The thermotropic material is modelled as a thin sheet of a matrix material containing a second material of discrete, spherical particles. Normal incident radiation at a single wavelength is imposed on the sheet and the transmittance and reflectance of the sheet is evaluated by a ray tracing algorithm. When the index of refraction of the matrix and particles are equal, the model simulates the thermotropic material in the clear state. When the refractive indices differ, the model simulates the translucent state. In subsequent sections, the governing equations of the model will be discussed in detail as well as the Monte Carlo method used to solve the model. The validation of the

model, which was compared to a simplified analytical solution and to experimental measurements, will also be discussed.

Nomenclature

a	radius of scattering domain (nm)
f_v	volume fraction of scattering domains (%)
I	radiative intensity ($W/m^2/sr$)
L	sheet thickness (mm)
l_σ	path length travelled by ray (mm)
m	relative index of refraction
$n_{particle}$	refractive index of scattering domains material
n_{matrix}	refractive index of matrix material
N	total number of rays used in Monte Carlo simulation
N_r	number of rays reflected
N_t	number of rays transmitted
Q_s	scattering efficiency factor
R_σ	random number used to determine the path length
R_θ	random number used to determine the scattering angle
R_ψ	random number used to determine the azimuth
$\hat{\mathbf{s}}$	unit vector describing direction of ray
$\hat{\mathbf{s}}_\mathbf{i}$	unit vector describing direction of radiation before being scattered into $\hat{\mathbf{s}}$
x	size parameter
i, **j**, **k**	global coordinate frame
θ	scattering angle (radians or degrees)
λ	wavelength of incident radiation (nm)
$\bar{\rho}$	sheet reflectance (%)
ρ	interface reflectivity
σ_s	scattering coefficient (mm^{-1})
τ_L	optical thickness
$\bar{\tau}$	sheet transmittance (%)
Φ	scattering phase function
ψ	azimuth angle (radians or degrees)
Ω	Solid angle (sr)

2. Model

The thermotropic material is modelled as a sheet (fig. 1) with uniform thickness L. The sheet is irradiated on the $z = 0$ interface at normal incidence with monochromatic radiation at wavelength λ. The sheet contains monodispersed, homogenously distributed, spherical particles with radius a and index of refraction $n_{particle}$ at a volume fraction f_v. The particles are embedded in a matrix material with index of refraction n_{matrix}. It is assumed that neither the matrix nor the particles absorb radiation. Independent scattering by the particles is also assumed. The assumption of independent scattering has implications for the range of f_v for which the model is valid. When the ratio of the average distance between particles and λ is less than 0.5, radiation scattered by a particle may be affected by neighboring particles [15]. For the range of particle sizes and the incident wavelength considered in the present study, the ratio is equal to 0.5 at $f_v \approx 10\%$ [15].

At the interface of the sheet with the surrounding media (air), radiation can be reflected or transmitted, due to a difference in refractive index of the air and the sheet. Inside the sheet, the radiation propagates until incident upon an embedded particle. The particle scatters radiation. Because no absorption within the media is assumed, the process of scattering and internal reflections is repeated, as shown in fig. 1, until the radiation is either transmitted through the sheet (the radiation exits through $z = L$ interface) or reflected out of the sheet (radiation exits through the $z = 0$ interface). If the radiation is reflected at an interface, specular reflection is assumed. In this case the choice of diffuse or specular reflection at the interface is arbitrary because the reflectivity is determined through the Fresnel equations regardless of whether diffuse or specular reflection is assumed.

The process of radiative scattering and reflection inside the sheet is governed by the equation of radiative transfer (RTE). The RTE is an integral-differential equation which describes the change in radiative intensity I along the direction of propagation $\hat{\boldsymbol{s}}$. For a non-absorbing, non-emitting media irradiated with monochromatic radiation, the RTE is:

$$\frac{dI}{ds} = -\sigma_s I + \frac{\sigma_s}{4\pi}\int_{\Omega_i}^{4\pi} I(\hat{s}_i)\Phi(\hat{s}_i, \hat{s})d\Omega_i \,. \qquad (1)$$

The first term on the right hand side of eq. (1), the product of the scattering coefficient σ_s and radiative intensity I, represents the radiative intensity scattered out of $\hat{\boldsymbol{s}}$. Physically σ_s is the inverse of the mean free path length travelled by a ray of radiation before being scattered. The second term is the radiative intensity scattered into $\hat{\boldsymbol{s}}$ from all other directions $\hat{\boldsymbol{s}}_i$. The integrand of the second term includes the scattering phase function Φ which describes the probability that radiation from $\hat{\boldsymbol{s}}_i$ will be scattered into $\hat{\boldsymbol{s}}$.

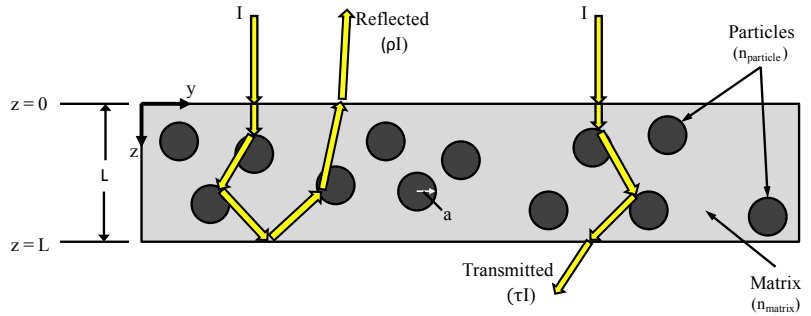

Fig. 1. Model of a thermotropic sheet of thickness L with scattering domains of radius a. Incident radiation can be reflected by the interfaces and scattering domains or transmitted

The RTE is often expressed in terms of a dimensionless variable, the optical thickness. The overall optical thickness τ_L of a non-absorbing material with homogeneous distributed particles of constant radius a is:

$$\tau_L = \sigma_s L = \frac{3}{4}\frac{f_v Q_s}{a} L, \tag{2}$$

where Q_s of eq. (2) is the scattering efficiency factor of the particle. Under the assumptions that the particles scatter independently and that the matrix material does not absorb radiation, Q_s and Φ are determined by Mie theory. Mie theory is a solution to Maxwell's equations for an electromagnetic wave that is incident upon a *single* spherical particle embedded in non-absorbing media [16]. Q_s and Φ are functions of two dimensionless parameters: the relative index of refraction m

$$m = \frac{n_{particle}}{n_{matrix}}. \tag{3}$$

and the size parameter x:

$$x = \frac{2\pi a}{\lambda}. \tag{4}$$

The Fresnel equations provide the boundary conditions, the transmissivity and reflectivity of the interface, for the RTE. The complexity of the RTE prohibits analytical solutions except for simplified cases [15]. In the present study, a statistical method, a collision Monte Carlo technique [15, 17], is used to solve the RTE. The paths of many individual rays (10^5 – 10^7) must be tracked to obtain statistically relevant results.

The program algorithm begins by launching a ray at normal incidence at the $z = 0$ interface (fig. 1). At the interface, the reflectivity of the interface and the probability of the ray being reflected are calculated by applying the Fresnel equations for normal incidence. If the ray is reflected, the reflectance count N_r is incremented and a new ray is launched. If the ray is transmitted through the $z = 0$ interface, the path length l_σ travelled by the ray is determined by random number R_σ by:

$$l_\sigma = \frac{1}{\sigma_s}\ln\left(\frac{1}{R_\sigma}\right). \tag{5}$$

If the path length is less than the thickness of the sheet, then the ray is scattered and the scattering angle θ is found by inverting:

$$R_\theta = \frac{1}{2}\int_{\theta'=0}^{\theta} \Phi(\theta')\sin\theta' \, d\theta'. \tag{6}$$

The inversion of eq. (6) is obtained through numerical integration at intervals of ~1.5°. Scattered angles within the integration interval are determined by linear interpolation, and Φ is calculated by the Mie scattering program BHMIE [16]. The azimuth angle ψ is determined by random number R_ψ:

$$\psi = 2\pi R_{\psi} . \quad (7)$$

Together θ and ψ describe the new direction of the ray after being scattered. After the new direction is determined, a new l_σ is calculated, and the position vector is updated. The scattering algorithm of equations (5) to (7) is repeated until the projection of the position vector on the z-axis is greater than the sheet thickness or less than zero at which point the ray must have intersected an interface.

When a ray intersects an interface, another random number is generated. If the generated random number is less than the transmissivity of the interface, the ray is transmitted through the interface. The transmittance count N_t is incremented when a ray is transmitted through the z = L interface. Similarly, the reflectance count N_r is incremented when a ray is transmitted through the z = 0 interface. After N rays, reflectance $\overline{\rho}$ and transmittance $\overline{\tau}$ of the sheet are determined:

$$\overline{\rho} = \frac{N_r}{N} ; \quad \overline{\tau} = \frac{N_t}{N} . \quad (8)$$

In the following section, the results of the Monte Carlo simulation are presented and compared to experimentally measured data to validate the model. Two parameters are held constant for all simulation runs: the incident radiation wavelength is 550 nm to correspond to the peak of the solar spectrum and the index of refraction of the matrix is 1.50 to be representative of the refractive index of polymers. The sheet thickness, particle size, index of refraction of the particle, and volume fraction of particles are varied to correspond to the experimental sample. For each data point, $5x10^5$ – $1x10^6$ rays were tracked such that the standard deviation was less than 1% for each simulation.

3. Model validation

To validate the model, model predictions are compared with: (1) the analytical solution for a sheet of non absorbing, non-scattering media, and (2) measured transmittance for 0.3 mm thick polymer samples containing particles with 200 nm radius at m ranging from 0.97 to 1.09 and f_v ranging from 5 to 18.2%.

The analytical derivation and solution for the reflectance and transmittance of a sheet of non-absorbing, non-scattering (m = 1 or f_v = 0) media is well known [15]. For n = 1.50, the analytical transmittance and reflectance are 92.3% and 7.7%, respectively. The model for m = 1 agrees with the analytical solution by also predicting $\overline{\tau}$ = 92.3% and $\overline{\rho}$ = 7.7%.

In the experimental validation, samples with a matrix of polyvinyl acetate (PVA) (n_{matrix} = 1.47 at room temperature), a thickness of 0.3 mm +/- 0.02 mm, and 200nm radius scattering domains were prepared. Relative indices of refraction of 0.966, 1.016, and 1.088 were obtained by using scattering domains of silica, poly (methyl methacrylate) (PMMA), and polystyrene (PS) at f_v = 9.6 % +/- 0.5%. Samples with PS scattering domains were also fabricated at volume fractions of 5, 13.5, and 18.2%. Since $m \neq 1$, the samples represent a thermotropic material that has changed to the translucent state. All samples were prepared by preparing an aqueous emulsion of PVA and scattering domains. The mixture was allowed to equilibrate for one hour before one gram of the mixture was spread onto a 3.8 cm diameter form. The sample was then allowed to dry on the form at ambient temperature in a fume hood for 20 hours. The normal-hemispherical, spectral transmittance and reflectance of the samples were measured, from 250 to 2400 nm, using a Lambda 1050 spectrophotometer equipped with a 150mm integrating sphere. The solar weighted normal-hemispherical transmittance was calculated with an air mass (AM) of 1.5 by:

$$\bar{\tau}_{sol} = \frac{\int_{250}^{2400} \tau_\lambda E_\lambda d\lambda}{\int_{250}^{2400} E_\lambda d\lambda} . \quad (9)$$

Figure 2 shows transmittance as a function of m for the predicted values from the Monte Carlo simulation for a wavelength of 550 nm, the measured normal-hemispherical transmittance at 550 nm, and the measured solar weighted transmittance. The volume fraction is held constant at 9.6%. The measured transmittance at 550 nm has a maximum of 85% at m =1 As the mismatch in refractive indices increases (m < 1 or m > 1), the transmittance decreases. For example at m = 1.088, the measured transmittance at 550 nm is 50%. The predictions of the simulation match well with the measured values at 550 nm: the difference between the model prediction and the measured values is within the experimental error (typically < +/-2%). Because the model assumes no absorption, the transmittance predictions are greater than the measured values. The only discrepancy is the control of m = 1: the model predicts a transmittance of 92% and the measured transmittance at 550 nm is 84%. The difference in transmittance between predicted and measured for the m = 1 case may be caused by a combination of absorption and imperfections (such as inhomogeneity and particle aggregation) within the sample.

Figure 3 shows transmittance as a function of f_v. The measured transmittance at 550 nm decreases with increasing f_v from 60% at f_v = 5% to 50% at f_v = 13.5%. The measured transmittance does not decrease from f_v = 13.5% to f_v = 18.2%. The model accurately predicts the transmittance at 550 nm except for the case of f_v = 18.2 %. At f_v = 18.2%, the model of 200 nm particles predicts a lower transmittance than was measured. This discrepancy at the largest volume fraction considered is attributed to particle aggregation. As shown in the figure, when the model is run with an aggregate radius of 900 nm, corresponding to x = 10, the predicted transmittance is very close to the measured value. The size of the aggregate was estimated using scanning electron microscopy and subsequent particle analysis with ImageJ software.

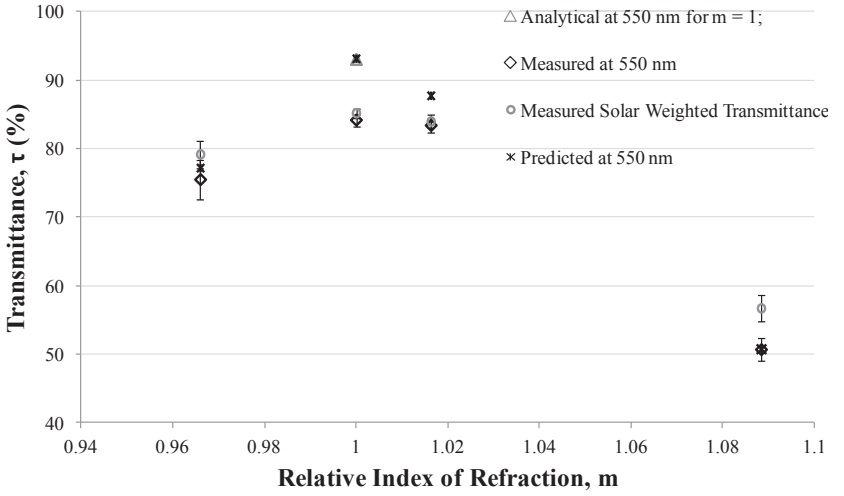

Fig. 2. Model predictions compared to measured values for samples with fv = 9.6%, a = 200 nm, and L = 0.3mm. The model consistently predicts the transmittance at 550 nm and predicts the trends that the solar weighted transmittance follows

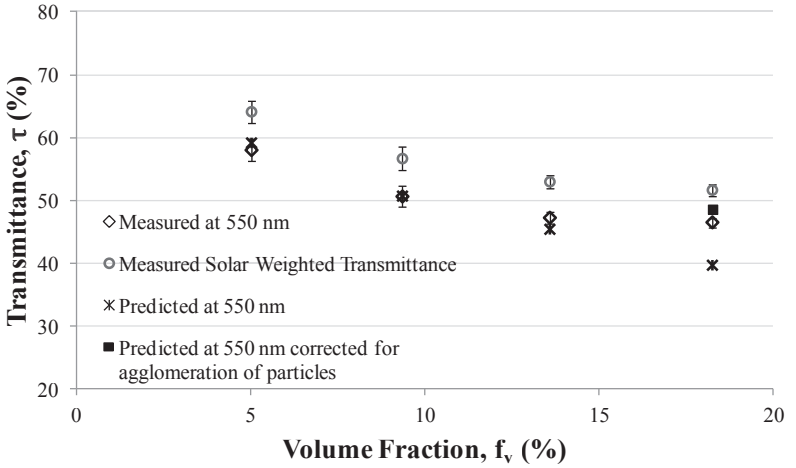

Fig. 3. Model predictions compared to measured values for samples with $m = 1.088$, $a = 200$ nm, and $L = 0.3$mm. The model consistently predicts the transmittance at 550 nm and predicts the trends that the solar weighted transmittance follows for volume fractions less than 13.5%

Because the Monte Carlo simulation requires 10^6 ray tracking iterations to predict radiative performance at a single wavelength, there is a significant computational benefit if it can be shown that model predictions at 550 nm wavelength are comparable to solar weighted transmittance data. As shown in fig. 2 and 3, the model accurately predicts the *trends* for the solar weighted transmittance data. The model predictions are less than the measured solar weighted transmittance for $f_v \leq 13.5\%$. For example for $f_v = 13.5$ % and $m = 1.088$, the model predicts a transmittance of 45% while the solar weighted transmittance is 52%. For the combinations of m and f_v studied, the difference between the model prediction at 550 nm and the solar weighted transmittance is approximately 6-8%.

4. Summary and future work

Thermotropic materials offer the potential for low cost, passive overheat protection because their temperature dependent optical properties. These materials are composed of a matrix material in which a second material, referred to as the scattering domain, is dispersed. Ideally, below the switching temperature, the refractive indices of the matrix and dispersed material are equal and the transmittance is high. Above the switching temperature, approximately the melting temperature of the scattering domain, the refractive indices of the two materials differ and a portion of the incident radiation is scattered, reducing the transmittance. In the present study, a model for the transmittance and reflectance of thermotropic materials is described. The thermotropic material is modelled as a sheet with monodispersed, homogenously distributed, spherical particles. The sheet is irradiated at normal incidence with monochromatic radiation at wavelength λ. It is assumed that (1) the spherical particles scatter radiation independently and (2) neither the particles nor the matrix absorbs radiation. Transmittance and reflectance of the sheet are found by a Monte Carlo statistical solution in which the path of the incident ray is tracked. The intent of the model is to investigate the effect of particle size and volume fraction, the relative index of refraction (between the particle and matrix) and the sheet thickness on the reflectance $\overline{\rho}$ and transmittance $\overline{\tau}$.

The model was validated through comparison with the analytic solution for a non absorbing sheet and with transmittance data for thin polymer sheets with embedded spherical particles. There is good

agreement between the model predictions and transmittance data obtained for a range of m and f_v (a and L constant). Transmittance was reduced significantly from approximately 90% to 50%, when the mismatch in refractive index was approximately 9% (from m= 1 to m=1.088 respectively). Model predictions of transmittance for an incident wavelength of 550 nm are 6-8% less than the solar weighted transmittance data. Future work entails obtaining model runs for a wide range of optical thickness, size parameters and relative index of refractions. By using these dimensionless parameters to characterize the thermotropic material, a configuration that minimizes transmittance can be achieved (given the limitations of the materials and processes that are available).

Acknowledgements

This work was supported through grants from the Institute for Renewable Energy (at the University of Minnesota) and the Environment and the National Renewable Energy Laboratory.

References

[1] "Task 39 - Polymeric Materials for Solar Thermal Applications, Solar Heating & Cooling Program, IEA. http://www.iea-shc.org/task39/index.html,".

[2] Burch, J., Merrigan, T., Jorgensen, G., 2006, "Low-Cost Residential Solar Thermal Systems," . http://www1.eere.energy.gov/solar/review_meeting/pdfs/p_68_burch_nrel.pdf

[3] Merrigan, T., 2007, "Solar Heating & Lighting: Solar Water Heating R&D - DOE Solar Energy Technologies Program," . http://www1.eere.energy.gov/solar/review_meeting/pdfs/shl_1_merrigan_nrel.pdf.

[4] 2011, "NREL Solar Thermal Research Objective," June 2012. http://www.nrel.gov/solar/

[5] Resch, K., Hausner, R., and Wallner, G. M., 2009, "All Polymeric Flat-Plate Collector — Potential of Thermotropic Layers to Prevent Overheating," pp. 561-565.

[6] Resch, K., and Wallner, G. M., 2009, "Thermotropic Layers for Flat-Plate collectors—A Review of various Concepts for Overheating Protection with Polymeric Materials," Solar Energy Materials and Solar Cells, **93**(1) pp. 119-128.

[7] Nitz, P., and Hartwig, H., 2005, "Solar Control with Thermotropic Layers," Solar Energy, **79**(6) pp. 573-582.

[8] Seeboth, A., Ruhmann, R., and Muehling, O., 2010, "Thermotropic and Thermochromic Polymer Based Materials for Adaptive Solar Control," Materials, **3**(12) pp. 5143-5168.

[9] Jahns, E., 1999, "Crosslinked Polymer Systems having Reversible Temperature-Dependent Radiation Transmission," (5977201) .

[10] Muehling, O., Seeboth, A., Haeusler, T., 2009, "Variable Solar Control using Thermotropic core/shell Particles," Solar Energy Materials and Solar Cells, **93**(9) pp. 1510-1517.

[11] Raicu, A., Wilson, H. R., Nitz, P., 2002, "Facade Systems with Variable Solar Control using Thermotropic Polymer Blends," Solar Energy, **72**(1) pp. 31-42.

[12] Nitz, P., Ferber, J., Stangl, R., 1998, "Simulation of Multiply Scattering Media," Solar Energy Materials and Solar Cells, **54**(1-4) pp. 297-307.

[13] Dombrovsky, L. A., Randrianalisoa, J. H., and Baillis, D., 2007, "Infrared Radiative Properties of Polymer Coatings Containing Hollow Microspheres," International Journal of Heat and Mass Transfer, **50**(7–8) pp. 1516-1527.

[14] Dombrovsky, L., 2005, "Modelling of Thermal Radiation of Polymer Coating Containing Hollow Microspheres," High Temperature, **43**(2) pp. 247-258.

[15] Modest, M., 2003, "Radiative Heat Transfer," Academic Press, pp. 822.

[16] Bohren, C.F., and Huffman, D.R., 1998, "Absorption and Scattering of Light by Small Particles," Wiley-Interscience, pp. 530.

[17] Farmer, J.T., and Howell, J.R., 1998, "Advances in Heat Transfer," Elsevier, pp. 333-429..